Identifying the future water and salinity risks to irrigated viticulture in the Murray-Darling Basin, South Australia

V. Phogat[a,b,*], J.W. Cox[a,c], J. Šimůnek[d]

[a] South Australian Research and Development Institute, GPO Box 397, Adelaide, SA, 5001, Australia
[b] CCS Haryana Agricultural University, Hisar, 125 004, India
[c] The University of Adelaide, PMB1 Glen Osmond, SA, 5064, Australia
[d] Department of Environmental Sciences, University of California, Riverside, CA, 92521, United States

ARTICLE INFO

ABSTRACT

Water and water related salinity risks to viticulture were assessed by running the HYDRUS-1D model with 100 ensembles of downscaled daily meteorological data obtained from the Global Climate Model (GCM) for 2020–2099. The modeling output was evaluated for seasonal irrigation requirements of viticulture (I_r), root zone soil salinity at the beginning of the new season (EC_{swi}), and the average seasonal salinity (EC_{sw}) for all 100 realizations for four 20-year periods centred on 2030 (2020–2039), 2050 (2040–2059), 2070 (2060–2079), and 2090 (2080–2099). The model showed a 4.2% increase in the mean seasonal I_r of viticulture during 2020–2039 as compared to I_r of 350.9 mm during 2004–2015. Similarly, the mean seasonal I_r increased by 7.5, 10.9, and 16.9% during 2040–2059, 2060–2079, and 2080–2099, respectively, as compared to 2004–2015. These projections indicate that viticulture can face significant deficit conditions, which may have a drastic impact on the sustainability and productivity of the grapevine. Likewise, the average median EC_{swi} increased by 40% during 2020–2039 as compared to the 2004–2015 mean EC_{swi} value of 1.63 dS/m, but remained below the threshold ($EC_{sw} = 4.2$ dS/m) for viticulture. The median seasonal EC_{swi} almost doubled (3.15 dS/m) during 2040–2059, varied from 1.73–8.15 dS/m during 2060–2079, and increased more than three times during 2080–2099 to surpass the threshold salinity for grapevines. Similarly, the seasonal average root zone salinity (EC_{sw}) showed a 47% increase during 2020–2039 over the baseline salinity. It continued increasing at a growing pace during 2040–2059 (1.5–8.64 dS/m) and 2060–2079 (2.78–9.52 dS/m), and increased to almost three times (6.04 dS/m) during 2080–2099 compared to the corresponding baseline salinity (1.97 dS/m). The continued presence of high salt concentrations in the root zone can significantly affect the growth, yield, and wine quality. The modeling results indicate that soil salinity at the beginning of the vine season and the average seasonal salinity are crucial factors that may need special management to sustain the viticulture in this region.

1. Introduction

Water availability and climate change have played a crucial role in the story of human development. The lack of available water for agricultural production, energy projects, other forms of anthropogenic water consumption, and ecological use is already a major issue in many parts of the world that is expected to grow more severe with increasing population, higher food demand, rising temperatures, and changing precipitation patterns (Elliott et al., 2014). Climate change is expected to have a significant impact on various economic sectors (IPCC, 2014) but especially on agriculture because crops are heavily influenced by weather conditions during their life cycles (Bernetti et al., 2012). Future projections foresee that climate change could reduce plant water availability and increase agricultural area under drought, affecting crop production (Collins et al., 2013). A rise in temperatures, for instance, could lead to soil moisture deficits and a growing risk of vegetation desiccation due to increased evapotranspiration and decreased soil moisture (Goyal, 2004; Riediger et al., 2014). On the other hand, increased CO_2 concentrations in the atmosphere may provide an enhanced opportunity for higher carbon assimilation by crops and lead to an increase in the crop yield (Wang et al., 2012), provided that other inputs are not limiting the crop growth. Ecological and economic consequences of climate change on agricultural ecosystems are expected to vary widely depending on the spatial patterns of land cover, land use practices, and regional climate variability (Bindi and Olesen, 2011; Iglesias et al., 2012).

* Corresponding author at: South Australian Research and Development Institute, GPO Box 397, Adelaide, SA, 5001, Australia.
  E-mail addresses: vinphogat@gmail.com, vinod.phogat@sa.gov.au (V. Phogat).

Australia has the largest area under arid and semi-arid climate in the world, with about 80% of the country receiving rainfall of less than 600 mm per year (Mushtaq et al., 2013). South Australia represents one of the driest regions in Australia. Climate models expect a 10–20% reduction in cold season rainfall in much of the southern Australia (CSIRO and BoM, 2016). A greater volatility in weather patterns is also projected, particularly more frequent and more severe droughts (CSIRO and BoM, 2016). South Australia is a major grape and wine producing region in Australia, contributing 48% of the total wine grape crush. 92% of vineyards in South Australia use supplementary drip irrigation (ABS, 2015). The South Australian (SA) part of the Murry-Darling basin (Riverland) is the largest grapevine producing region, accounting for 61% of the South Australian production and 28% of the national production (Hayman and McCarthy, 2013). Climate change projections for the Riverland show drier and hotter conditions, with an 11.4–21.7% decrease in annual rainfall, a 1.9–3.6 °C increase in maximum temperatures, and a 1.5–3.1 °C increase in minimum temperatures by the turn of the 21st century (Charles and Fu, 2015). These projections can have a dramatic impact on river flow conditions, water allocation in the Riverland, and the future security of the quantity and quality of irrigation water for the irrigated horticulture including viticulture.

Water requirements of the viticulture production in the Riverland region are met almost exclusively by irrigation from the Murray River. The extent of flow in the river decides the volume of water allocations to irrigated industries. Given the economic importance of grapevine in the region, a high seasonal variability of rainfall and water allocations, and an imminent prospect of climate change, it is critical to assess the future irrigation demand and related risks to viticulture. Reduced flows in the Murray River and associated restricted irrigation may result in increased root zone salinity to the detriment of wine quality. Even if rainfall levels are unaffected, the risk of intense droughts will increase due to the augmentation of the atmospheric evaporative demand as a result of warming (Alcamo et al., 2007). Increased temperatures coupled with reduced rainfall may increase the salt accumulation in upper soil layers and hence affect plant growth (Cullen et al., 2009). It is essential to understand the impact of future climate drivers on irrigation requirements and soil salinity so that appropriate adaptation and mitigation strategies can be adopted for sustainable viticulture production.

Grapevine growth is sensitive to various environmental factors, including atmospheric CO_2 concentrations, air temperatures, and water availability (Salazar-Parra et al., 2010), and is thus vulnerable to climate change (Fraga et al., 2014; Kizildeniz et al., 2015). The most critical impact of climate change observed at the global scale is the advancement of maturity of grapes by 4–8 days (Jones et al., 2005; Webb et al., 2011). Webb et al. (2007) projected a 50-day advancement in the maturity of grapes in the Coonawarra region of South Australia by 2050. The effects of global warming and associated changes in precipitation patterns may alter terroirs (White et al., 2009), i.e., unique combinations of climate and soils that are used to produce wines of distinctive styles (Webb et al., 2012). However, the information on the future irrigation requirements of viticulture and the magnitude of other related risks (salinity) in the soil is sparse. A number of modeling studies have attempted to evaluate the effects of climate change on water use in agriculture for other crops (Fischer et al., 2007; Elgaali et al., 2007; De Silva et al., 2007; Xiong et al., 2010; Gondim et al., 2012; Save et al., 2012; Lee and Huang, 2014; Woznicki et al., 2015). Most of these studies showed an increase in the irrigation demand for typical annual crops. However, a majority of these studies were performed using a low resolution data (e.g., monthly temperature and precipitation data) and the impact of climate change on the irrigation demand was only examined for a small number of scenarios that may not have captured the wide variability and uncertainty in the projections of climate models. Using only a limited number of ensembles of Global Climate Model (GCM) projections may result in a limited understanding of plausible future climate scenarios, unreliable projections of the future, and

consequently poor decision-making and adaptation (Gohari et al., 2013).

There is a large number of models (e.g., https://soil-modeling.org/resources-links/model-portal/model-collection; Vereecken et al., 2016) that have been used in similar studies as ours. All these models have their own pros and cons depending on their capabilities of addressing climate, soil, and crop variables for the future climate. Among these, HYDRUS-1D (Šimůnek et al., 2016) is one of the models that has been most widely used for solving a wide range of irrigation related problems (see https://www.pc-progress.com/en/Default.aspx?h1d-references), including those similar to ours. The key characteristics and recent developments of HYDRUS-1D can be found in its technical manual and published literature (e.g., Šimůnek et al., 2016). The main features of HYDRUS-1D that are required in our study include an option to trigger irrigation when a prescribed pressure head is reached at a specified soil depth, to evaluate root water uptake as a function of soil water content and daily potential transpiration, and to consider the coupled transport of water and solutes in the soil. HYDRUS-1D can also calculate surface runoff, evaporation, and infiltration fluxes for atmospheric boundary conditions, and drainage fluxes through the bottom of the soil profile. Hence, HYDRUS-1D was selected to conduct the long-term simulations for identifying future risks to irrigated viticulture.

This modeling study involves 100 ensembles of GCM projections and considers a wide range of uncertainty in climate variables. Irrigation requirements are evaluated using the HYDRUS-1D numerical model and a fine temporal resolution (daily) of climatological data. The goal of this study is to understand how the irrigation demand of viticulture is impacted by climate change and what unforeseen impacts (e.g., salinity) could arise due to the variability in the water use. Understanding the impacts of climate change should help in effectively adapting to it and mitigating its effects for sustainable viticulture.

2. Materials and methods

2.1. Description of the study area

The South Australian Murray-Darling Basin region (Riverland) covers 56,703 square kilometers or about 7% of the state's land area (Fig. 1). The landscape varies from the low-lying coastal plains to the flat lands of the Mallee. The Murray River is a dominant and influential feature of the region due to the importance of its waters for irrigated agriculture and the environment and in meeting domestic, livestock, and industrial needs. It supports a wide range of flora, fauna, natural environments, and human activities. Most irrigated industries are spread along the Murray River corridor of about 10 km on either side. The region's climate can be characterized as Mediterranean, experiencing hot, dry summers and cold, wet winters.

The Riverland is famous in Australia for irrigated perennial horticulture and viticulture production. The productivity and sustainability of vineyards are fully dependent on the water allocation from the Murry River. However, water flow in the Murray River is highly erratic and dependent on the extent of rainfall in the eastern high reaches, which feed the river system. During drought years, the water allocation is significantly reduced; for example, during 2006–07 the water allocation was only 18% of the total allocation. Hence, inadequate rainfall has a direct impact on flow conditions in the Murray River, and South Australia is usually impacted the most, being on the tail end of the basin.

To undertake the long term (2015–2099) modeling study for evaluating future water requirements of viticulture and salinity dynamics in the soils, the Loxton Research Centre (34.44°S and 140.59°E) was selected as a representative site. It has the typical Riverland climate and falls within the central part of the viticulture production region. The climate parameters were obtained from the Bureau of Meteorology for Loxton, which is about 1 km away from the study site. Annual average rainfall and reference crop evapotranspiration (ET_0) during the last
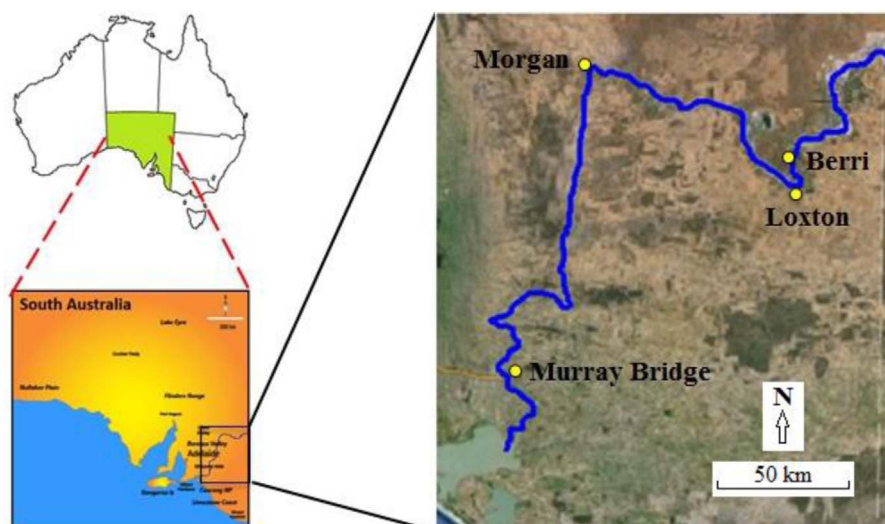
100 years amounted to 265 and 1369 mm, respectively, which indicates a strong need for irrigation for crop production.

Prior to conducting the long-term simulations on future climate, the model was run on the current climate (1st July 2004–30th June 2015) data for the study site. This was done to stabilize the initial conditions for the long-term simulations and to compare the current climate results with the future climate projections.

2.2. Soil characteristics

The soils in the study area (Riverland) are characterized by the presence of light-textured Aeolian deposits at the soil surface, underlain by a heavy-textured soil at variable depths. These soils are known as Duplex soils (Chittleborough, 1992), which covers a large cultivated area in Australia and are present is significant extent in the Riverland. However, there exists a huge variability of soils at different locations in the Riverland (Hall et al., 2009). The light-textured surface soils (0–30 cm) are predominately composed of sand particles with only a small clay content (sand 90–94%, clay 5.5–9%, and silt 0.5–1.3%; Hall et al., 2009), whereas the soils at lower depths (below 30 cm) contain appreciable amounts of clay content (20–40%). The soil texture at the study site varies from a sandy loam topsoil (0–30 cm) overlying a sandy clay loam subsoil (30–100 cm). The organic carbon content in the soil varies from 0.3 to 1.14%, being higher in the surface soil, and pH increases from 7.8 to 8.1 from the soil surface to the 1 m depth. The soil hydraulic parameters used in modeling were estimated from the particle size distribution and bulk density data from the study site. The soil hydraulic parameters used in this investigation are given in Table 1. Similar hydraulic parameters have also been used in other related studies (Phogat et al., 2016, 2017) in the Riverland where HYDRUS has been calibrated and validated for spatiotemporal water content distribution in the soil under viticulture.

2.3. Model description

The HYDRUS-1D software can simulate one-dimensional variably-saturated water flow, heat movement, and transport of solutes involved in sequential first-order decay reactions (Šimůnek et al., 2016). The governing one-dimensional water flow equation is described as follows:

$$\frac{\partial \theta}{\partial t} = \frac{\partial}{\partial z}\left(K(h)\frac{\partial h}{\partial z} + K(h)\right) - S\ (h, h_s, z, t) \tag{1}$$

where θ is the soil water content ($L^3 L^{-3}$), t is the time (T), h is the soil water pressure head (L), h_s is the osmotic head (L), z is the vertical coordinate (positive upwards) (L), $K(h)$ is the unsaturated hydraulic conductivity function (LT^{-1}), and $S(h,h_s,z,t)$ is the sink term accounting for an actual volume of water uptake by plant roots from a unit volume of soil per unit of time ($L^3 L^{-3} T^{-1}$). Water extraction $S(h,h_s,z,t)$ from the soil is computed according to the Feddes macroscopic approach (Feddes et al., 1978). In this method, the potential transpiration rate, T_p, is distributed over the root zone using the normalized root density distribution function and multiplied by the dimensionless water and salinity stress response functions. Hence, this model evaluates plant root water uptake rates based on the local soil water and osmotic pressure heads at any point in the root zone. Potential transpiration (T_p) is reduced below its potential value when the soil is no longer capable of supplying the amount of water required by the plant under the prevailing climatic conditions. Potential root water uptake is further reduced by the osmotic stress, resulting from the salinity of irrigation water and the presence of salts in the soils. The effect of water and salinity stresses was assumed to be multiplicative so that different stress response functions could be used for water and salinity stresses. Critical values of pressure heads for root water uptake were taken from previous investigations on grapevine (Phogat et al., 2017) in the study area. The threshold and slope model parameters were obtained from the previous regional study (Zhang et al., 2002) evaluating salinity thresholds (EC_e = 2.1 dS/m) and percent reductions (12.8%) in different root stocks of grapevine.

The temporal and spatial distribution of soil solution salinity (EC_{sw}) was modeled as a non-reactive solute (e.g., Ramos et al., 2011; Wang et al., 2014; Phogat et al., 2014). These studies demonstrated that this approach could be successfully used in environments under intensive irrigation and fertigation management. The longitudinal dispersivity was assumed to be one tenth of the modeling domain (Cote et al., 2003) and the molecular diffusion coefficient for salts in water was considered to be 1.66 cm²/day (Phogat et al., 2014, 2017). Since it is difficult to predict changes in the river water quality under the future climate change, the EC_{iw} data for irrigation water was based on the water

Table 1
Soil hydraulic parameters used in the modeling study.

Textural layers	Soil depth (cm)	Bulk density (g cm^{-3})	Soil hydraulic parameters					
			θ_r (cm^3 cm^{-3})	θ_s (cm^3 cm^{-3})	α (cm^{-1})	n	K_s (cm day^{-1})	l
Sandy loam	0–30	1.6	0.05	0.37	0.031	1.94	120.81	0.5
Sandy clay	30–100	1.5	0.07	0.41	0.02	1.26	14.14	0.5

quality analysis conducted by the Murray Darling Basin Authority at Berri during 2004–2015. Since the measured EC_{iw} values for several irrigation schedules were missing, the average measured value of EC_{iw} (0.3 dS/m) during the 2004–2015 period was considered in all modeling simulations. The average salinity of rainfall in the Mildura region, which is close to the SA Riverland, has been reported as 0.12 dS/m (Cresswell et al., 2010) and was adapted in the present modeling investigation.

2.4. Irrigation scheduling

The trigger irrigation option available in HYDRUS-1D (Dabach et al., 2013) was used to generate irrigation schedules for grapevine. Irrigation is triggered when the predefined suction level in the soil profile is reached, the timing of which depends on the daily climate conditions, plant water requirements, soil texture, and water availability in the soil profile. Typically, irrigation is triggered using tensiometers, which are widely used for irrigation scheduling, including in vineyards. Tensiometers measure the suction (pressure head) at the point where the ceramic porous cup is placed in the soil and irrigation is applied when the suction (e.g., 60 kPa for grapevines) is reached. Similarly, in HYDRUS-1D, when the suction in the soil reaches the trigger value (e.g., 60 kPa), the irrigation of specified duration (5.5 h) and rate (4.364 cm/day) is automatically applied. Total amount of irrigation thus applied (10 mm/day/event) is similar to the amount normally applied to grapevine in the Loxton region (ICMS, 2007). The trigger point in this study was located at a 30-cm soil depth, which is similar to other field (Soar and Loveys, 2007) and modeling (Phogat et al., 2017) studies in this region and coincides with the maximum root activity for viticulture. Other studies also used a similar suction for irrigating grapevines (Edwards and Clingeleffer, 2013) at a 30-cm soil depth for well-watered conditions. The use of the same trigger irrigation option used for current climate (2004–2015) matched the water budget guidelines for 100% yield of grapevine in the Riverland (ICMS, 2007).

2.5. Domain depth and initial conditions

The simulation domain depth was selected based on the maximum rooting depth of grapevine (100 cm) reported in the literature and previous modeling studies on grapevine in the study area (e.g., Phogat et al., 2017). Measured values from the experimental site were used as the initial conditions for water content and soil solution salinity (EC_{sw}) for current climate (2004–2015). However, the terminal (30th June 2015) water (0.09–0.28 cm^{3}cm^{-3}) and EC_{sw} (0.68–2.35 dS/m) values for the current climate were imposed as initial condition for the future climate (1st July 2016–30th June 2099) simulations. These values provide a link between the modeling of future climate scenarios and the current climate. The upper boundary condition for water flow was set to atmospheric conditions with surface runoff, and the bottom boundary condition was set to free drainage. The concentration flux boundary condition was used at both top and bottom boundaries for solute transport.

All simulations were performed on a daily basis from 1st July 2015 to 30th June 2099 for all 100 ensembles of downscaled climate data. However, the modeling outputs of irrigation requirements and root zone salinity dynamics have been reported from 1st July 2019 to 30th June 2099 to align it with the 20-year periods (2020–2039, 2040–2059, 2060–2079, and 2080–2099) of future climate projections (Charles and Fu, 2015).

2.6. Climatic parameters for modeling

The input parameters for HYDRUS-1D for the future climate scenarios were developed from a set of downscaled projections generated by the Goyder Institute for Water Research for South Australia (Charles and Fu, 2015). These projections were downscaled from a suite of

global climate model (GCM) projections for six climate variables: rainfall, maximum and minimum temperature, areal potential evapotranspiration (APET), solar radiation, and vapor pressure deficit. The projections were obtained for intermediate and high emission scenarios, i.e., for representative concentration pathways RCP4.5 and RCP8.5, respectively. Since the climate projections have a strong variability, 100 stochastic datasets were generated by the downscaling model (NHMM) for different GCMs. Rather than selecting a few ensembles of a suite of models, as usually done in many studies (Fischer et al., 2007; Xiong et al., 2010; Gondim et al., 2012; Save et al., 2012; Lee and Huang, 2014; Woznicki et al., 2015), we adopted all 100 ensembles of a better performing model (Charles and Fu, 2015) so that the uncertainty in climate projections can be adequately addressed in modeling scenarios. The GCM (GFDL ESM2 M) data downscaled for RCP8.5 for Loxton in the Riverland were used in the current modeling study to consider the worst-case scenario for the water related risks to viticulture. Daily APET and rainfall data for the simulation period (2015–2099) were used to develop input parameters for the HYDRUS-1D model.

A quick assessment of seasonal (1st July to 30th June) deviations in downscaled rainfall data for Loxton revealed a strong decreasing trend throughout the 21st century (Fig. 2). During the first 20-year period (2020–2039), a strong likelihood of drought conditions at Loxton during 2025, 2029, 2035 and 2039 seasons is projected (Fig. 3a), which shows that dry conditions often occur after every five years. Average rainfall during this period is projected to decline by 13.7% as compared to average rainfall during the last 100 years (1916–2015). Similarly, during the second 20-year period (Fig. 3b), the reduction in median rainfall increased to 17.8%, and by further 32.7% during the last quarter of the century. The projections showed that one-half of years (10 years) is expected to receive seasonal rainfall less than 200 mm during the second 20-year period (2040–2059). The second half of the 21st century is projected to have a more dramatic reduction in seasonal rainfalls. Especially during the 2080–2099 period, median rainfall plummeted to less than 200 mm (Fig. 3d).

Similarly, the variation in the seasonal APET among all 100 realizations downscaled for Loxton for all 20-year future periods is box plotted in Fig. 4. The seasonal median APET during the first 20-year period (2020–2039) ranged from 1332.8 to 1368.6 mm, which showed only a small reduction in the average median value (1356.6 mm) compared to the average seasonal reference crop evapotranspiration (ET_0 = 1369 mm) of the last 100 years, i.e., from 1916 to 2015. The maximum median seasonal APET was observed during 2039. Similarly, during the second 20-year period (2040–2059), the seasonal APET varied from 1273 to 1473 mm and the average median APET slightly increased (0.6%) as compared to the last 100 years APET. However, during the third (2060–2079) and fourth (2080–2099) 20-year periods, the average median APET increased by 2.5 and 5.0%, respectively, compared to the average 100-year value. Median seasonal APET of all
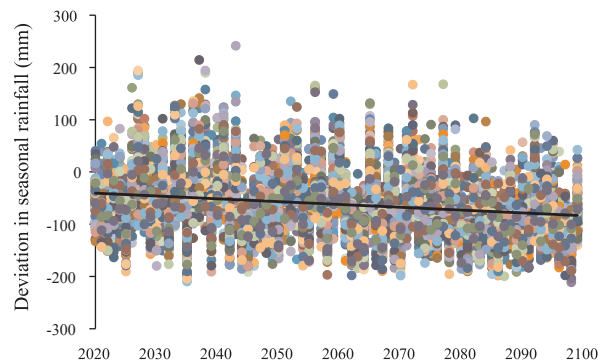

Fig. 2. Predicted deviations of seasonal (1st July to 30th June) rainfall from the historical mean value (265 mm) in 100 realizations of the downscaled GCM (GFDL ESM2 M) data for Loxton.
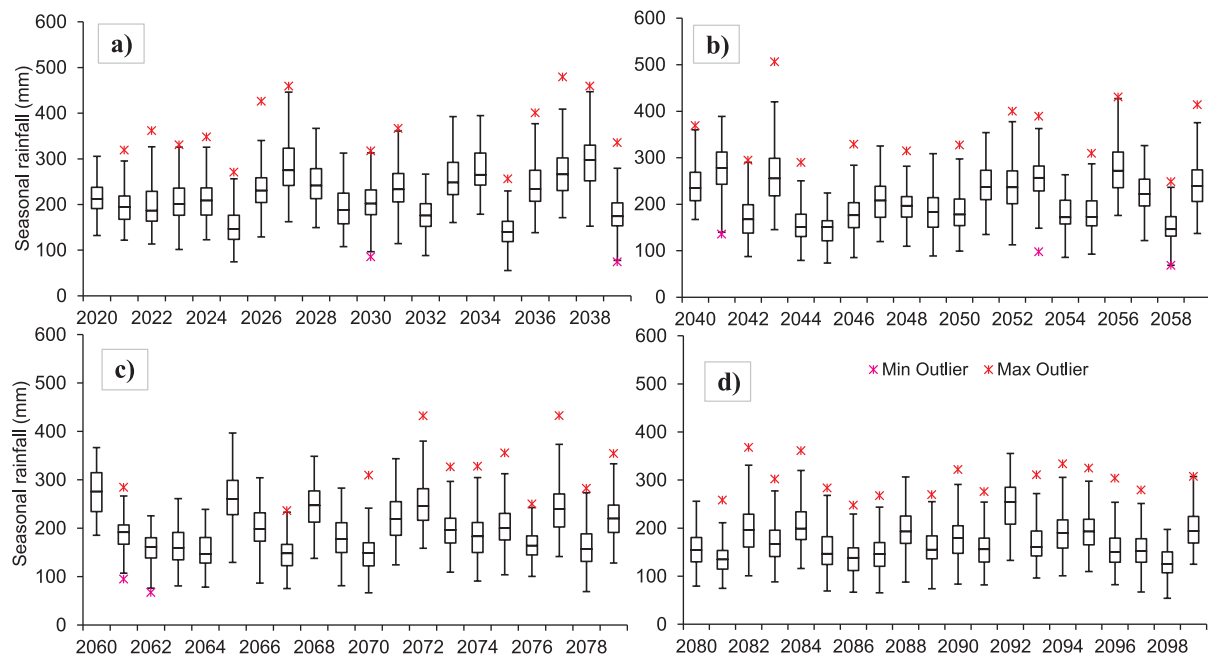
Fig. 3. Variability in seasonal rainfall (mm) at Loxton in 100 realizations of downscaled GCM data during a) 2020–2039, b) 2040–2059, c) 2060–2079, and d) 2080–2099 periods.

100 ensembles showed a linear increasing trend ($R^2 = 0.59$–0.74) during all 20-year time periods at Loxton.

Daily crop evapotranspiration (ET_C) of grapevine was then estimated (Allen et al., 1998) using daily APET values and local crop coefficients (K_c). The K_c coefficients for grapevine for local conditions were obtained from the Irrigation Recording and Evaluation System (IRES) developed by the Crop Management Service (Rural Solutions SA, 2011). The leaf area index (LAI) for grapevine was taken from Nguyen et al. (2013), which was estimated in a local vineyard. Similar K_c and LAI values were adopted every year, assuming similar canopy and well-grown vine conditions. The values of daily potential evapotranspiration (ET_C) and LAI, along with daily rainfalls at the study site during the simulation period, were then used as time-variable boundary conditions in the model. 100 simulations of daily input data were used to run HYDRUS-1D and to simulate water requirements and salinity dynamics

in the soil from 1st July 2015 to 30th June 2099. However, the results reported below are in 20-year blocks (2020–2039, 2040–2059, 2060–2079, and 2080–2099) to align them with the climate projections. The model-triggered irrigation requirements (I_r) and the root-zone soil solution salinity at the beginning (September, EC_{swi}) and average seasonal root zone salinity (EC_{sw}) are processed on a seasonal basis (1st July–30th June) for all 100 simulations.

3. Results and discussion

3.1. Seasonal irrigation and salinity in the current climate

The data on seasonal irrigation (I_r) and average rootzone salinity (EC_{sw}) and salinity at the beginning of the season (EC_{swi}) for current climate is presented in Fig. 5. The amount of seasonal I_r varied from
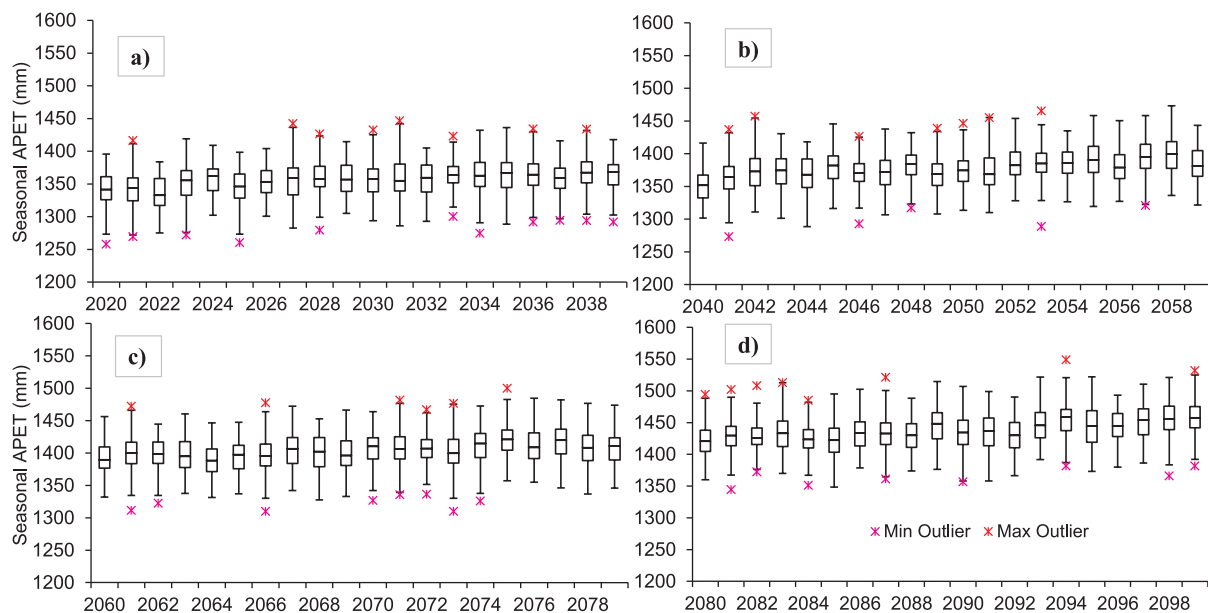

Fig. 4. Deviations in yearly (1st July to 30th June) areal potential evapotranspiration (APET) in 100 realizations of downscaled GCM data for Loxton during a) 2020–2039, b) 2040–2059, c) 2060–2079, and d) 2080–2099 periods.
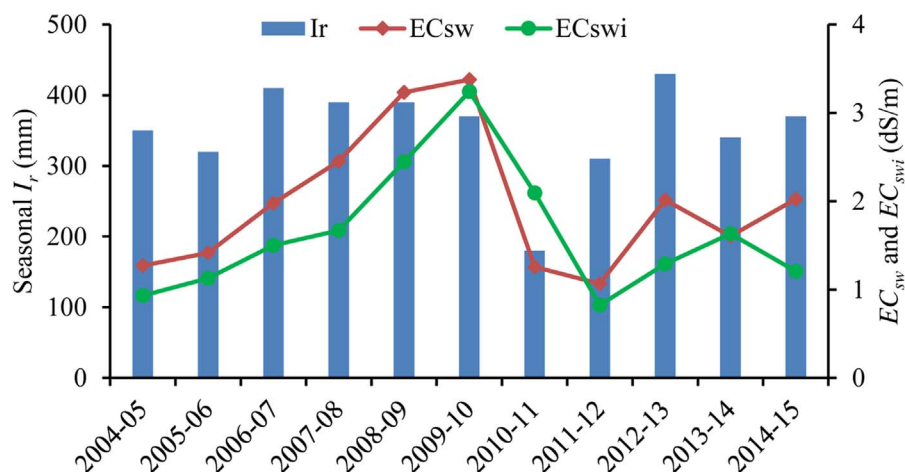
Fig. 5. Seasonal irrigation (Ir), soil solution salinity at the beginning (ECswi) and seasonal average (ECsw) during the current climate (2004–05 to 2014–15).

180–430 mm and being higher during the less rainfall years (2006–2009). However, the average root zone salinity (EC_{sw} and EC_{swi}) showed an increasing trend as during the same period. It shows that extent of seasonal rainfall had tremendous impact on the root zone salinity dynamics irrespective of normal irrigation application. When the drought condition broke during 2010 and annual rainfall (542 mm) exceeded more than double of 100 years average, the irrigation requirement drastically reduced and remained half of the 11 years average (330.9 mm) leading to a decrease in soil salinity. Notably, most of the rainfall in the study area is received during winter season which may generate higher leaching fraction due to less evapotranspiration demand and hence greater salt leaching effect. Cucci et al. (2016) also found similar impact of winter season rainfall under the Mediterranean climate in a sandy loam soil. Overall, the seasonal salinity and average salinity (1.97 dS/m) during the entire period of current climate (2004–2015) remained below threshold (EC_{sw} = 4.2 dS/m) for viticulture.

3.2. Future irrigation requirement for viticulture

The extent of variability in the seasonal irrigation requirements (I_r) of viticulture during the 2020–2039 period projected by the model for 100 different yearly realizations of meteorological data is presented in the box-plots in Fig. 6a. The seasonal I_r is in close agreement with projected seasonal rainfall (Fig. 3). The median I_r values fluctuated similarly as rainfall received during the season. The median seasonal I_r during 2025, 2032, 2035, and 2039 increased by 9, 6, 9, and 6%, respectively, compared to the average median I_r of 366 mm. Unavailability of water for irrigation during these crucial intermittent dry years can have a significant impact on the growth and yield of grapevine and the wine quality. On the other hand, the reduction in seasonal I_r during high rainfall years (2027, 2028, 2034, and 2038) ranged between 7 and 10% compared to the average median I_r. Overall, the mean seasonal I_r during 2020–2039 increased by 4.2% compared to the corresponding I_r requirement of 350.9 mm during 2004–2015. Deviations in the seasonal I_r were estimated by subtracting the average seasonal I_r (350.9 mm) during 2004–2015 from the seasonal I_r for each ensemble in different years (Fig. 7). The data showed that there was a slightly declining trend among yearly mean values of I_r over this period (Fig. 7a).

During 2040–2059, the seasonal irrigation requirements of viticulture at Loxton were projected to vary from 260 to 460 mm in all ensembles. However, the median seasonal I_r remained mostly higher than the current value (350.9 mm), except during few low I_r seasons (2041 and 2056) (Fig. 6b). During this period, the average median seasonal water requirement of viticulture increased by 7.5% compared to the current requirement for 2004–2015. The seasonal irrigation requirements I_r were low in 2041 and 2056, which were wetter years that

received higher rainfall than the mean of 265 mm of the past 100 years at Loxton. The projected increase in the irrigation requirements during this period is much higher than the corresponding values observed during the previous 20-year period (Fig. 7b) because below average rainfall was projected by the climate models during this time. The maximum projected outlier was 460 mm, which is 30% more than the mean current baseline value. However, the minimum outlier may plummet as low as 260 mm. Hence, there exists a wide variability in the seasonal I_r for viticulture during this period. These scenarios indicate that viticulture can face significant deficit conditions. This may have a dramatic impact on the sustainability and productivity of the viticulture in the region.

The simulated yearly seasonal I_r of viticulture at Loxton during 2060–2079 varied from 240 to 480 mm, showing a 100% variability in different realizations (Fig. 6c). The average median seasonal I_r increased by 10.9% compared to the corresponding current baseline value (350.9 mm). Simulated seasonal I_r for viticulture again showed a strong relationship with the seasonal rainfall at Loxton. For example, high rainfall years (2060, 2065, 2072, and 2077), which normally occur every five years, had relatively lower water requirements. Conversely, the irrigation requirement of viticulture increased during low seasonal rainfall years (2064, 2067, 2070, 2076, and 2078). Deviations in the seasonal I_r over the baseline in different realizations showed an increasing trend over the years during this period (Fig. 7c).

Similarly, I_r continued to increase during the last 20-year (2080–2099) period of the 21st century (Fig. 6d). The seasonal I_r varied from 280 to 500 mm, and the average median I_r increased by 16.9% compared to the current baseline irrigation requirement. The occurrence of drought years during this period is projected to be more frequent and longer lasting compared to previous decades. Hence, water requirements of viticulture were also projected to increase in the same fashion. For example, the periods during 2080–2081, 2086–2087, 2091, 2093, and 2096–2098 are projected to have higher irrigation requirements. Even in the 2092 year, which had the lowest projected median I_r (380 mm) of this period, it was 8.3% higher than the current baseline value (350.9 mm). The deviations of seasonal I_r from the current I_r also showed an increasing trend over the years, which means that water requirements are expected to increase during this period (Fig. 7d).

The seasonal I_r for each ensemble and year is plotted in Fig. 8 against the corresponding seasonal rainfall to highlight the degree of correlation between these two values. The seasonal I_r showed a linear relationship (R^2 = 0.56–0.66) with seasonal rainfall during all 20-year periods. The seasonal I_r decreased linearly with an increase in the amount of rainfall received during the same period, indicating a strong dependence of irrigation requirements on rainfall. The modeling results indicated a continued upsurge of the water demand for irrigation for
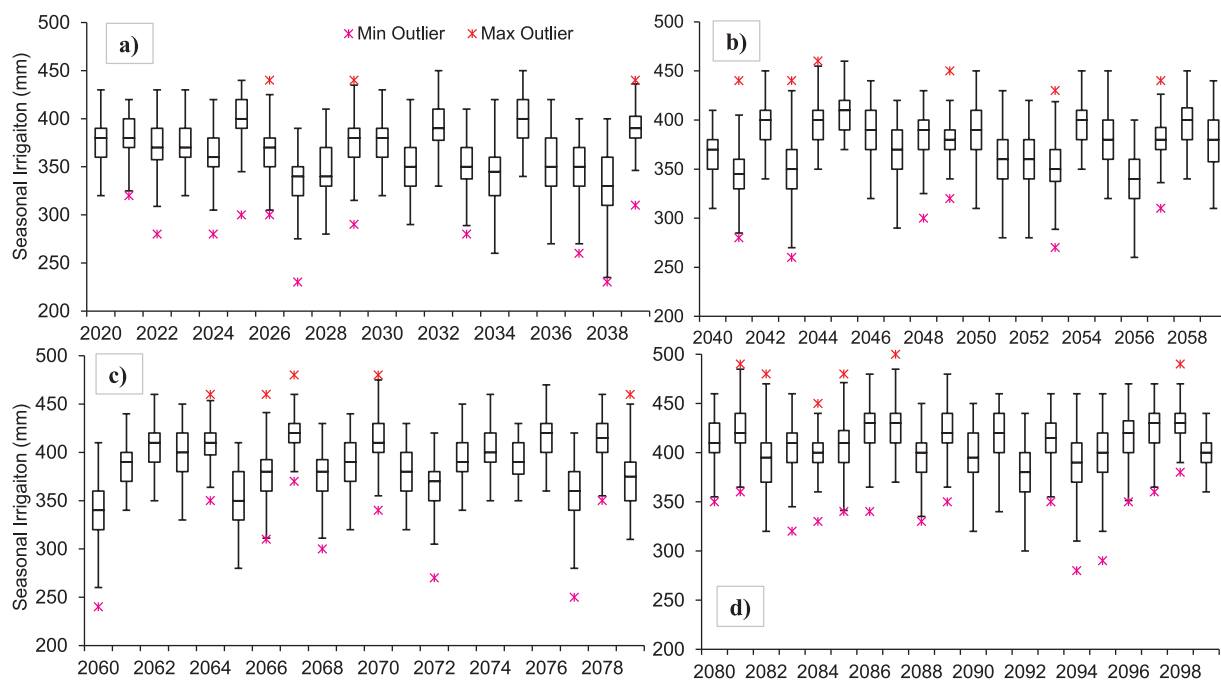
Fig. 6. Predicted variability in the seasonal irrigation requirement (I_r) for viticulture at Loxton during the a) 2020–2039, b) 2040–2059, c) 2060–2079, and d) 2080–2099 periods.

viticulture during the whole 21st century in response to a reduction in seasonal rainfall. Hence, water security could be an important issue for ensuring the viticulture production under the projected climate change. Therefore, water deficit conditions or low water allocations during the viticulture growing season can pose a significant threat to the sustainability of grapevine in the Riverland.

3.3. Impact of climate change on root zone salinity dynamics

The root zone salinity at the beginning of the new viticulture season (EC_{swi}) in September during the 2020–2039 period showed a gradual increase over the years (Fig. 9a) despite irrigations being triggered at a required pressure (60 kPa). However, there was a slight reduction in the median EC_{swi} during 2034, which coincided with higher rainfall during two preceding seasons and when the occurrence of some high-intensity rains could have leached a fraction of root zone salts out of the crop root zone. But the EC_{swi} increased again during 2035, which was a comparatively dry year. Despite these seasonal salinity dynamics, the median root zone salinity remained below the crop threshold level (EC_{sw} = 4.2 dS/m, the blue line in Fig. 9) over the entire 20-year period (2020–2039), which indicates a low water-related salinity hazard during this period. However, some max outliers (see red crosses in
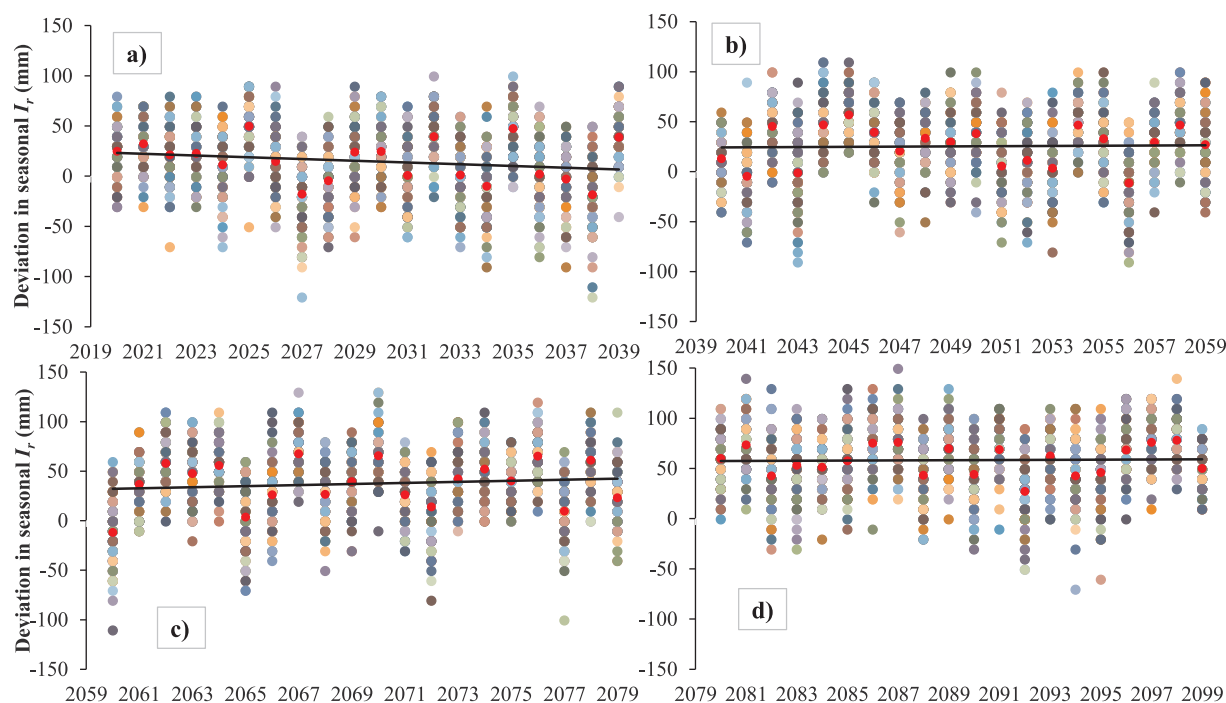

Fig. 7. Deviations in the model-predicted seasonal irrigation requirements of viticulture at Loxton from the mean baseline (2005–2015) value (350.9 mm) during the a) 2020–2039, b) 2040–2059, c) 2060–2079, and d) 2080–2099 periods.
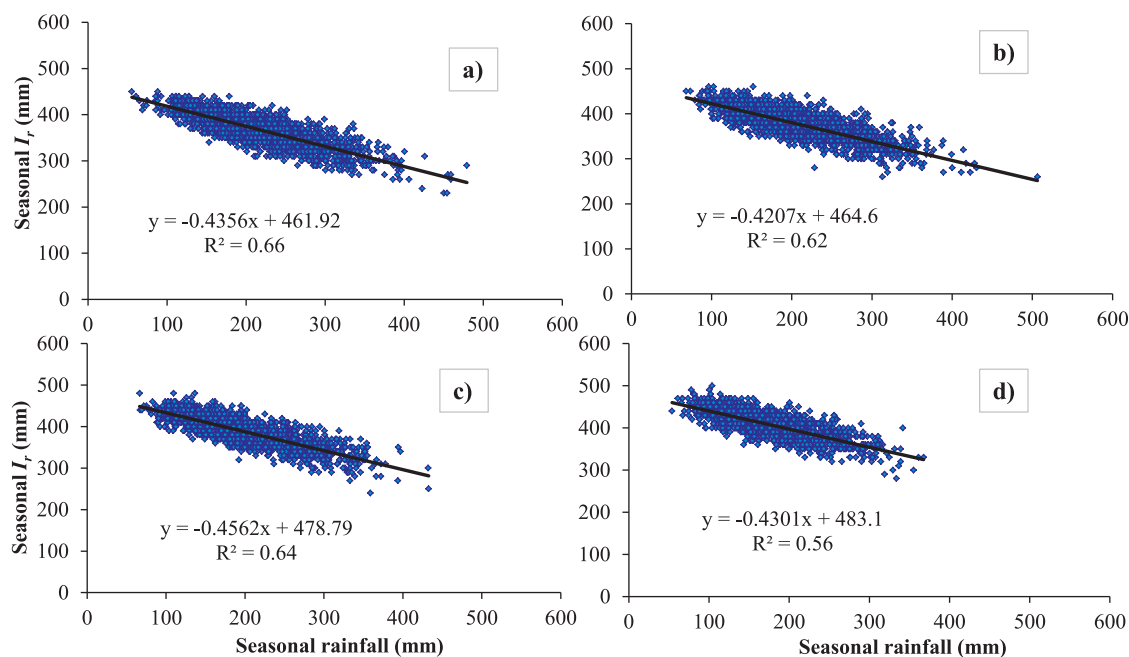
Fig. 8. The relationship between predicted seasonal I_r of viticulture and downscaled seasonal rainfall at Loxton during the a) 2020–2039, b) 2040–2059, c) 2060–2079, and d) 2080–2099 periods.
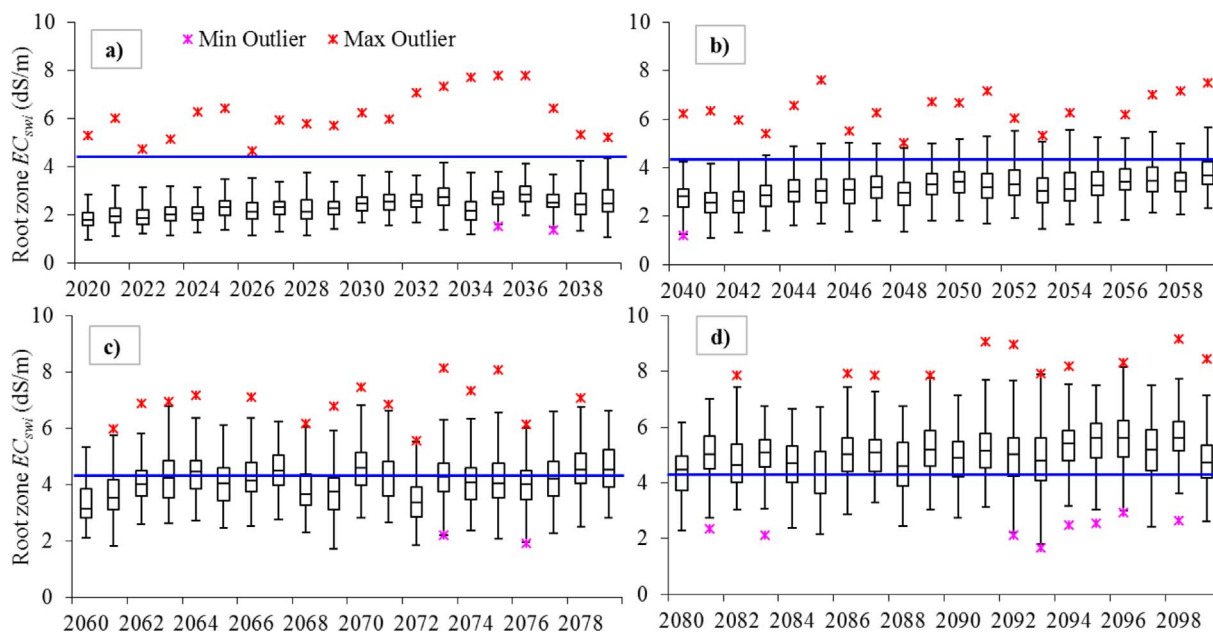

Fig. 9. Predicted variability in the root zone soil salinity at the beginning of the viticulture season (EC_{swi}) at Loxton during the a) 2020–2039, b) 2040–2059, c) 2060–2079, and d) 2080–2099 periods. The blue line represents the salinity tolerance threshold for viticulture. (For interpretation of the references to colour in this figure legend, the reader is referred to the web version of this article.)

Fig. 8a) showed EC_{swi} much higher than the threshold salinity. This situation (Av. $EC_{swi} > 4.2$ dS/m) occurred only in 1.7% of the realizations especially during drought conditions. Though, the average median EC_{swi} during the 2020–2039 period increased by 40% compared to the corresponding value of 1.63 dS/m during the baseline period (2004–2015), which indicates increased salts depositions in the root zone. However, a gradual reduction in rainfall (Figs. 2 and 3) over the years contributed to an increase in the root zone salinity. These salts can pose increasing risks to the vine growth and its sustainable production.

Similarly, the seasonal EC_{swi} during the 2040–2059 varied from 1.1 to 7.63 dS/m (Fig. 9b). The average median EC_{swi} almost doubled to

3.15 dS/m compared to the corresponding mean value during the baseline period (1.63 dS/m), indicating a significant salt deposition in the root zone. Only 10% of realizations showed seasonal EC_{swi} higher than the crop threshold during this period. These salts can pose a serious salinity-related threat to the vine growth and yield, and the wine quality. A tendency of salts to build up in the soil during this period (2040–2059) is related to consistently below-average rainfall, which was not sufficient to leach salts from the root zone. Isidoro and Grattan (2011) also found through modeling that rainfall distribution plays a major role in determining seasonal soil salinity in the root zone.

During 2060–2079, the seasonal EC_{swi} varied from 1.73 to 8.15 dS/m (Fig. 9c) and the overall average median EC_{swi} increased by 150%

compared to the average baseline value of 1.63 dS/m. This indicates that continued additions of salts into the soil through irrigation are not leached out of the root zone. Therefore, salt concentrations in the root zone increased above the crop threshold in 45% of climate realizations and increased the salinity risks to the irrigated viticulture in the Riverland.

Similarly, the seasonal EC_{swi} varied from 1.67 to 9.18 dS/m in various realizations during the final 20-year period (2080–2099) (Fig. 9d). This period showed a slight increase in the upper outliers as compared to the previous 20-year period. However, the average median EC_{swi} at the beginning of the season increased more than three times (5.0 dS/m) as compared to the corresponding salinity during the baseline period. The median EC_{swi} for the entire final 20-year period increased above the threshold salinity ($EC_{sw} = 4.2$ dS/m) of grapevine (Zhang et al., 2002) in 78% of climate realizations. High salinity at the beginning of the season can have a dramatic impact on the bud burst and initial growth, which can subsequently be reflected in vine growth such as the canopy development, berry development, ripening, harvesting, and the quality of the wine. The modeling results revealed that soil salinity at the beginning of the vine season is a crucial factor that needs special attention to ensure sustainable viticulture.

The average root zone salinity during the growing season (EC_{sw}) varied from 1.33–8.49 dS/m and showed an increasing trend during 2020–2039 (Fig. 10). The median EC_{sw} of 100 ensembles (2.21–3.26 dS/m) also showed an increasing trend with time, though it remained below the salinity threshold for viticulture (Fig. 10a). However, several outliers, which occurred due to drought conditions in some of the realizations that provided less opportunity for proper salt leaching from the root zone, showed a significantly higher EC_{sw}. The average median salinity was 47% higher than the corresponding baseline value (1.97 dS/m), which reflects increased salt depositions in the root zone. This suggests that the extent of rainfall and irrigation is not adequate for salt leaching under viticulture irrigated at the full requirement with good quality water. Increased salinity may hamper the adequate vine growth and can influence the berry production and wine quality.

The average salinity during the cropping season (EC_{sw}) showed a large variability among the yearly seasonal realizations as it varied from 1.5 to 8.64 dS/m during 2040–2059 (Fig. 10b). However, the

median EC_{sw} varied from 3.27 to 4.49 dS/m in different realizations and generally showed an increasing trend with time. The simulated median salinity is higher than the threshold (4.2 dS/m) in 35% of modeling realizations, which means that it can have a tremendous impact on the normal vine growth, yield, and the wine quality. Though the projected amount of seasonal irrigation showed an increasing trend during this period, irrigation was unable to generate necessary leaching to remove the salts from the root zone.

During 2060–2079, the seasonal EC_{sw} showed a significant variability and varied from 2.78 to 9.52 dS/m in different climate change realizations (Fig. 10c). The average median salinity (4.98 dS/m) increased almost two and half times compared to the corresponding value during the baseline period (2004–2015). Yearly median EC_{sw} values remained above the crop threshold in 81% of climate change realizations, indicating a strong likelihood of salt related problems. High values of upper outliers occurred during drought periods due to insufficient leaching because rainfall plays a key role in maintaining a proper salt balance in the crop root zone. High soil salinities during this period can damage the growing tissues and can significantly affect the growth, yield, and the sustainability of the viticulture.

The EC_{sw} continued to increase during the last 20-year period of the 21st century. It ranged from 2.98 to 10.44 dS/m in different yearly realizations (Fig. 10d). It is worth noting that EC_{sw} showed a much higher increasing trend during the last decade of the 21st century. EC_{sw} showed a strong correlation with a similar reduction in rainfall and an increase in the irrigation demand during this period. The average median seasonal EC_{sw} increased almost three times (6.05 dS/m) compared to the corresponding baseline value (1.97 dS/m) and remained higher than the viticulture salinity threshold (4.2 dS/m) in 97% of climate change realizations. Eventually, enhanced levels of salt concentrations in the root zone exert an increased osmotic impact and reduce vine water uptake by roots, which in turn influences many physiological processes of the plant such as transpiration, photosynthesis (Russo et al., 2009), stem and leaf water potential (Walker et al., 1981), stomatal conductance (Walker et al., 1981; Prior et al., 1992a), and net assimilation rate (Downton et al., 1990). Ultimately, negative impacts of increased salinity and water stresses on physiological traits are transmitted into the fruit yield reduction (Prior et al., 1992b; Stevens et al., 1999; Walker et al., 2002; DeGaris et al., 2015) and the
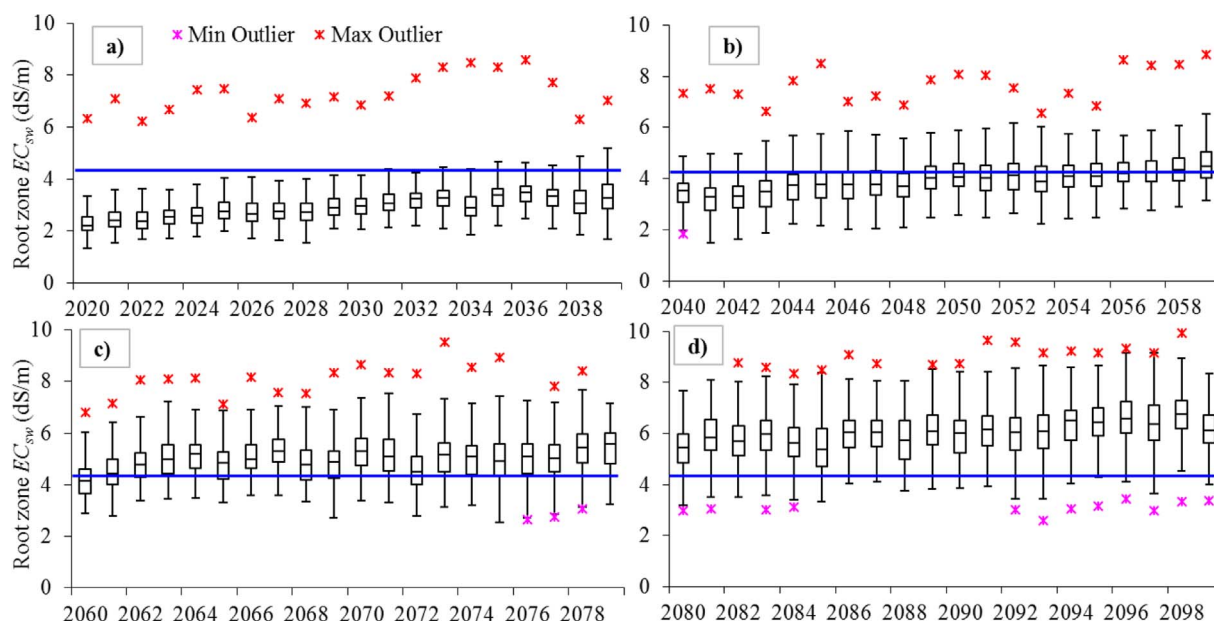

Fig. 10. Predicted variability in the seasonal average soil solution salinity in the root zone (EC_{sw}) of viticulture at Loxton during the a) 2020–2039, b) 2040–2059, c) 2060–2079, and d) 2080–2099. The blue line represents the salinity tolerance threshold for viticulture. (For interpretation of the references to colour in this figure legend, the reader is referred to the web version of this article.)

deterioration of the berry juice composition (Prior et al., 1992a; DeGaris et al., 2015) and wine quality. Sometimes, the concentration of individual ions such as Cl^- or Na^+ can increase to a toxic level and can disturb the plant metabolism (Munns and Tester, 2008). Nonetheless, increased root zone salinity above the crop threshold can be controlled by adopting an appropriate leaching fraction (LF) for salinity control. This could have been done, for example, by triggering irrigations at a lower suction than in current simulations (i.e., < 60 kPa). However, it is certain that adopting higher LF would further enhance the total irrigation requirement of viticulture under projected climate change in the study area.

It is worth mentioning that soluble salts that are leached out of the crop root zone may re-enter it in response to dynamic evaporative fluxes at the soil surface. Alternatively, these salts can leach deeper into the soil and may enter the river system via groundwater, which may be hydraulically connected, as reported in many previous studies (e.g. Cook et al., 2004; Tan et al., 2007). Maintaining a proper leaching fraction can help in leaching the salts from the crop root zone. Aragüés et al. (2014) reported an increase in salinity and sodicity in soil under sustained deficit irrigation of vineyards due to the reduction in the leaching fraction. However, a high leaching fraction may be needed in low rainfall areas where seasonal salinity can increase above the crop tolerance threshold. These results suggest that irrigation-induced salts can pose an increased threat to the normal growth and yield of grapevine, and can at the same time enhance the salinity related environmental risks to the river system.

4. Conclusions

In this study, a numerical model HYDRUS-1D was used to evaluate the water and water-related salinity risks to viticulture for 100 different downscaled ensembles of climate model (GFDL ESM2 M) projections. Such an assessment of the impact of climate change in all plausible scenarios of downscaled GCM projections can help in reducing the uncertainty in simulated outcomes of a model. The study suggests a strong likelihood of an increase in the irrigation demand of viticulture in the future. Seasonal irrigation requirements increased by 4.2% during the 2020–2039 period as compared to the baseline period (2004–2015). The irrigation-induced salinity risks were low during this period as the initial and seasonal average salinities in the soil remained below the crop threshold. However, the water allocation to the viticulture may be affected due to a reduction in rainfall (13.7%) and an increased occurrence of droughts projected by the climate model.

After that, model simulations showed continuously increasing irrigation requirements and increased salinity risks to viticulture in the following 20-year periods (2040–59, 2060–2079, and 2080–2099). The seasonal irrigation requirement (I_r) increased by 7.5, 10.9, and 16.9% during 2040–2059, 2060–2079, and 2080–2099, respectively. This large increase in the irrigation requirement was mainly associated with a reduction in rainfall projected by the climate models because a reduction in potential evapotranspiration was projected to be only 2.5 and 5% during 2060–2079 and 2080–2099, respectively. Model simulations also indicated a tremendous increase in the root zone salinity as rainfall-induced salt leaching was reduced to a great extent. The simulated seasonal average salinity increased three and four times compared to the base line and 81 and 97% of the climate ensembles showed a root zone salinity higher than the crop threshold during the 2060–2079 and 2080–2099 periods, respectively.

The study suggests that apart from an increase in the irrigation requirement, root zone salinity could be a much bigger problem to be faced by the irrigated viticulture in the Riverland region of South Australia and regions under similar climates around the world. If salts are not properly managed in a timely fashion, they can pose a serious risk for irrigated crops, including viticulture. These findings could help the stakeholders of irrigated viticulture in adopting strategies leading to the reduction in the salinity in the crop root zone.

References

ABS, 2015. Vineyards Estimates, Australia 2014–15, Cat. No. 1329. Australian Bureau of Statistics, Canberra.

Alcamo, J., Moreno, J.M., Nováky, B., Bindi, M., Corobov, R., Devoy, R.J.N., Giannakopoulos, C., Martin, E., Olesen, J.E., Shvidenko, A., 2007. Climate change impacts, adaptation and vulnerability. In: Parry, M.L., Canziani, O.F., Palutikof, J.P., van der Linden, P.J., Hanson, C.E. (Eds.), Contribution of Working Group II to the Fourth Assessment Report of the Intergovernmental Panel on Climate Change. Cambridge University Press, Cambridge, UK, pp. 541–580.

Allen, R.G., Pereira, L.S., Raes, D., Smith, M., 1998. Crop Evapotranspiration: Guidelines for Computing Crop Water Requirements. FAO Irrigation and Drainage Paper No. 56. FAO, Rome, Italy.

Aragüés, R., Medina, E.T., Clavería, I., Martínez-Cob, A., Faci, J., 2014. Regulated deficit irrigation, soil salinization and soil sodification in a table grape vineyard drip-irrigated with moderately saline waters. Agric. Water Manage. 134, 84–93.

Bernetti, I., Menghini, S., Marinelli, N., Sacchelli, S., Sottini, V.A., 2012. Assessment of climate change impact on viticulture: economic evaluations and adaptation strategies an analysis for the Tuscan wine sector. Wine Econ. Policy 1, 73–86.

Bindi, M., Olesen, J.E., 2011. The responses of agriculture in Europe to climate change. Reg. Environ Chang. 11, 151–158.

Charles, S.P., Fu, G., 2015. Statistically Downscaled Projections for South Australia –Task 3 CSIRO Final Report. Goyder Institute for Water Research Technical Report Series No. 15/1, Adelaide, South Australia.

Chittleborough, D.J., 1992. Formation and pedology of duplex soils. Aust. J. Exp. Agric. 32, 815–825.

Collins, M.R., Knutti, R., Arblaster, J., Dufresne, J.-L., Fichefet, T., Friedlingstein, P., Gao, X., Gutowski, W.J., Johns, T., Krinner, G., Shongwe, M., Tebaldi, C., Weaver, A.J., Wehner, M., 2013. Long-term climate change: projections, commitments and irreversibility. In: Stocker, T.F., Qin, D., Plattner, K., Tignor, M., Allen, S.K., Boschung, J., Nauels, A., Xia, Y., Bex, V., Midgley, P.M. (Eds.), Climate Change: the Physical Science Basis. Contribution of Working Group I to the Fifth Assessment Report of the Intergovernmental Panel on Climate Change. Cambridge University Press, Cambridge, United Kingdom and New York, NY, USA.

Cook, P.G., Leaney, F.W., Miles, M., 2004. Groundwater Recharge in the North-east Mallee Region, South Australia. Technical Report No. 25/04. CSIRO Land and Water, Adelaide.

Cote, C.M., Bristow, K.L., Charlesworth, P.B., Cook, F.J., Thorburn, P.J., 2003. Analysis of soil wetting and solute transport in subsurface trickle irrigation. Irrig. Sci. 22, 143–156.

Cresswell, R.G., Dighton, J., Leaney, F., Vleeshouwer, J., Morrow, D., Harris, M., Stenson, M., 2010. Australia-wide Network to Measure Rainfall Chemistry and Isotopic Composition –Final Report of Project MD311. CSIRO, Water for a Healthy Country National Research Flagship, Australia.

CSIRO, BoM, 2016. State of the Climate. Commonwealth Scientific and Industrial Research Organisation & Bureau of Meteorology (Accessed 28 August 2017). http://www.bom.gov.au/state-of-the-climate/State-of-the-Climate-2016.pdf.

Cucci, G., Lacolla, G., Mastro, M.A., Caranfa, G., 2016. Leaching effect of rainfall on soil under four-year saline water irrigation, Soil and. Water Res. 11, 181–189.

Cullen, B., Johnson, I., Eckard, R., Lodge, G., Walker, R., Rawnsley, R., McCaskill, M., 2009. Climate change effects on pasture systems in south-eastern Australia. Crop Pasture Sci. 60 (10), 933–942.

Dabach, S., Lazarovitch, N., Šimůnek, J., Shani, U., 2013. Numerical investigation of irrigation scheduling based on soil water status. Irrig. Sci. 31 (1), 27–36.

DeGaris, K.A., Walker, R.R., Loveys, B.R., Tyerman, S.D., 2015. Impact of deficit irrigation strategies in a saline environment on Shiraz yield, physiology, water use and tissue ion concentration. Aust. J. Grape Wine Res. 21, 468–478.

De Silva, C.S., Weatherhead, E.K., Knox, J.W., 2007. Predicting the impacts of climate change −a case study of paddy irrigation water requirements in Sri Lanka. Agric. Water Manage. 93, 19–29.

Downton, W.J.S., Loveys, B.R., Grant, W.J.R., 1990. Salinity effects on the stomatal behaviour of grapevine. New Phytol. 116, 499–503.

Edwards, E.J., Clingeleffer, P.R., 2013. Inter-seasonal effects of regulated deficit irrigation on growth, yield, water use, berry composition and wine attributes of cabernet sauvignon grapevines. Aust. J. Grape Wine Res. 19, 261–276.

Elgaali, E., Garcia, L.A., Ojima, D.S., 2007. High resolution modeling of the regional impacts of climate change on irrigation water demand. Clim. Change 84, 441–461.

Elliott, J., Deryng, D., Müller, C., Frieler, K., Konzmann, M., Gerten, D., Glotter, M., Flörke, M., Wada, Y., Best, N., Eisner, S., Fekete, B.M., Folberth, C., Foster, I., Gosling, S.N., Haddeland, I., Khabarov, N., Ludwig, F., Masaki, Y., Olin, S., Rosenzweig, C., Ruane, A.C., Satoh, Y., Schmid, E., Stacke, T., Tang, Q., Wisser, D., 2014. Constraints and potentials of future irrigation water availability on agricultural production under climate change. PNAS 111, 3239–3244.

Feddes, R.A., Kowalik, P.J., Zaradny, H., 1978. Simulation of Field Water Use and Crop Yield Simulation Monographs. Pudoc Wageningen, The Netherlands.

Fischer, G., Tubiello, F., van Velthuizen, H., 2007. Climate change impacts on irrigation water requirements: effects of mitigation, 1990–2080. Technol. Forecast Soc. Change 74, 1083–1107.

Fraga, H., Malheiro, A.C., Moutinho-Pereira, J., Jones, G.V., Alves, F., Pinto, J.G., Santos, J.A., 2014. Very high resolution bioclimatic zoning of Portuguese wine regions: present and future scenarios. Reg. Environ. Change 14, 295–306.

Gohari, A., Eslamian, S., Abedi-Koupaei, J., Bavani, A.M., Wang, D., Madani, K., 2013. Climate change impacts on crop production in Iran's Zayandeh-Rud River Basin. Sci. Total Environ. 442, 405–419.

Gondim, R.S., de Castro, M.A.H., Maia, A.D.N., Evangelista, S.R.M., Fuck, S.C.D., 2012. Climate change impacts on irrigation water needs in the Jaguaribe River Basin. J. Am. Water Resour. Assoc. 48 (2), 355–365.

Goyal, R.K., 2004. Sensitivity of evapotranspiration to global warming: a case study of arid zone of Rajasthan (India). Agric. Water Manage. 69, 1–11.

Hall, J.A.S., Maschmedt, D.J., Biling, N.B., 2009. The soil of Southern South Australia. The South Australian Land and Soil Book Series, vol. 1 Geological Survey of South Australia, Bulletin 56, Volume 1 Department of Water Land and Biodiversity Conservation, Government of South Australia.

Hayman, P., McCarthy, M., et al., 2013. Irrigation and drought in a southern Australian climate that is arid, variable, and changing. In: Schwabe, K. (Ed.), Drought in Arid and Semi-Arid Regions. Springer, Dordrecht, pp. 81–99.

ICMS (Irrigation and Crop Management Service), 2007. Water Budgeting Guidelines – Vines on the Upper Murray. Factsheet No. 15/06. Primary Industries and Resources South Australia, Govt. of South Australia.

Iglesias, A., Garrote, L., Quiroga, S., Moneo, M., 2012. A regional comparison of the effects of climate change on agricultural crops in Europe. Clim. Change 112, 29–46.

IPCC, 2014. Intergovernmental Panel on Climate Change. Climate Change 2014: Impacts, Adaptation, and Vulnerability. (Accessed 15 July 2017). http://www.ipcc.ch/report/ar5/wg2.

Isidoro, D., Grattan, S.R., 2011. Predicting soil salinity in response to different irrigation practices, soil types and rainfall scenarios. Irrig. Sci. 29, 197–211.

Jones, G.V., White, M.A., Cooper, O.R., Storchmann, K., 2005. Climate change and global wine quality. Clim. Change 73, 319–343.

Kizildeniz, T., Mekni, I., Santesteban, H., Pascual, I., Morales, F., Irigoyen, J.J., 2015. Effects of climate change including elevated CO_2 concentration, temperature and water deficit on growth water status, and yield quality of grapevine (*Vitis vinifera* L.) cultivators. Agric. Water Manage. 159, 155–164.

Lee, L., Huang, W.C., 2014. Impact of climate change on the irrigation water requirement in Northern Taiwan. Water 6, 3339–3361.

Munns, R., Tester, M., 2008. Mechanisms of salinity tolerance. Ann. Review Pl. Biol. 59, 651–681.

Mushtaq, S., Maraseni, T.N., Reardon-Smith, K., 2013. Climate change and water security: estimating the greenhouse gas costs of achieving water security through investments in modern irrigation technology. Agric. Syst. 117, 78–89.

Nguyen, T.T., Fuentes, S., Marschner, P., 2013. Effect of incorporated or mulched compost on leaf nutrient concentrations and performance of *Vitis Vinifera* cv. Merlot. J. Soil Sci. Pl. Nutr. 13 (2), 485–497.

Phogat, V., Šimůnek, J., Skewes, M.A., Cox, J.W., McCarthy, M.G., 2016. Improving the estimation of evaporation by FAO-56 dual crop coefficient approach under subsurface drip. Agric. Water Manage. 178, 189–200.

Phogat, V., Skewes, M.A., Cox, J.W., Sanderson, J., Alam, J., Šimůnek, J., 2014. Seasonal simulation of water, salinity and nitrate dynamics under drip irrigated mandarin (*Citrus reticulata*) and assessing management options for drainage and nitrate leaching. J. Hydrol. 513, 504–516.

Phogat, V., Skewes, M.A., McCarthy, M.G., Cox, J.W., Šimůnek, J., Petrie, P.R., 2017. Evaluation of crop coefficients, water productivity, and water balance components for wine grapes irrigated at different deficit levels by a sub-surface drip. Agric. Water Manage. 180, 22–34.

Prior, L.D., Grieve, A.M., Cullis, B.R., 1992a. Sodium-chloride and soil texture interactions in irrigated field-grown Sultana grapevines. 1. Yield and fruit-quality. Aust. J. Agric. Res. 43, 1051–1066.

Prior, L.D., Grieve, A.M., Cullis, B.R., 1992b. Sodium-chloride and soil texture interactions in irrigated field-grown Sultana grapevines–2. Plant mineral-content, growth and physiology. Aust. J. Agric. Res. 43, 1067–1083.

Ramos, T.B., Šimůnek, J., Goncalves, M.C., Martins, J.C., Prazeres, A., Castanheira, N.L., Pereira, L.S., 2011. Field evaluation of a multicomponent solute transport model in soils irrigated with saline waters. J. Hydrol. 407, 129–144.

Riediger, J., Breckling, B., Nuske, R.S., Schröder, W., 2014. Will climate change increase irrigation requirements in agriculture of Central Europe? A simulation study for Northern Germany. Environ. Sci. Eur. 26, 18. http://dx.doi.org/10.1186/s12302-014-0018-1. (Accessed 28 August 2017).

Rural Solutions SA, 2011. Irrigation and Crop Management Service, IRES Software, Version 4.0. Loxton Research Centre, Loxton, SA Australia.

Russo, D., Laufer, A., Silber, A., Assouline, S., 2009. Water uptake, active root volume and solute leaching under drip irrigation: a numerical study. Water Resour. Res. 45, W12413. http://dx.doi.org/10.1029/2009WR008015.

Salazar-Parra, C., Aguirreolea, J., Sánchez-Díaz, M., Irigoyen, J.J., Morales, F., 2010. Effects of climate change scenarios on Tempranillo grapevine (*Vitis vinifera* L.) ripening: response to a combination of elevated CO_2 and temperature and moderate drought. Plant Soil 337, 179–191.

Save, R., de Herralde, F., Aranda, X., Pla, E., Pascual, D., Funes, I., Biel, C., 2012. Potential changes in irrigation requirements and phenology of maize, apple trees and alfalfa under global change conditions in Fluvia watershed during XXIst Century: results from a modeling approximation to watershed-level water balance. Agric. Water Manage. 114, 78–87.

Šimůnek, J., van Genuchten, M. Th., Šejna, M., 2016. Recent developments and applications of the HYDRUS computer software packages. Vadose Zone J. 15 (6). http://dx.doi.org/10.2136/vzj2016.04.0033.

Soar, C.J., Loveys, B.R., 2007. The effect of changing patterns in soil moisture availability on grapevine root distribution, and viticultural implications for converting full-cover irrigation into a point-source irrigation system. Aust. J. Grape Wine Res. 13, 1–13.

Stevens, R.M., Harvey, G., Partington, D.L., Coombe, B.G., 1999. Irrigation of grapevines with saline water at different growth stages–1. Effects on soil, vegetative growth, and yield. Aust. J. Agric. Res 50, 343–355.

Tan, K., Berens, V., Hatch, M., Lawrie, K., 2007. Determining the Suitability of In-stream Nanotem for Delineating Zones of Salt Accession to the River Murray: A Review of Survey Results from Loxton, South Australia. Cooperative Research Centre for Landscape Environment and Mineral Exploration, Report 192. (pp. 24).

Vereecken, H., Schnepf, A., Hopmans, J.W., Javaux, M., Or, D., Roose, T., Vanderborght, J., Young, M.H., Amelung, W., Aitkenhead, M., Allison, S.D., Assouline, S., Baveye, P., Berli, M., Brüggemann, N., Finke, P., Flury, M., Gaiser, T., Govers, G., Ghezzehei, T., Franssen, H.J.H., Heppell, J., Horn, R., Huisman, J.A., Jacques, D., Jonard, F., Kollet, S., Lafolie, F., Lamorski, K., Leitner, D., Mcbratney, A., Minasny, B., Montzka, C., Nowak, W., Pachepsky, Y., Padarian, J., Romano, N., Roth, K., Rothfuss, Y., Rowe, E.C., Schwen, A., Šimůnek, J., Tiktak, A., Van Dam, J., van der Zee, S.E.A.T.M., Vogel, H.J., Vrugt, J.A., Wöhling, T., Young, I.M., Tiktak, A., 2016. Modeling soil processes: review, key challenges, and new perspectives. Vadose Zone J. 15 (5), 1–57. http://dx.doi.org/10.2136/vzj2015.09.0131.

Walker, R.R., Blackmore, D.H., Clingeleffer, P.R., Correll, R.L., 2002. Rootstock effects on salt tolerance of irrigated field-grown grapevines (*Vitis vinifera* L. cv Sultana), Yield and vigour inter-relationships. Aust. J. Grape Wine Res. 8, 3–14.

Walker, R.R., Torokfalvy, E., Scott, N.S., Kriedemann, P.E., 1981. An analysis of photosynthetic response to salt treatment in *Vitis vinifera*. Aust. J. Pl. Physiol. 8, 359–374.

Wang, D., Heckathorn, S.A., Wang, X.Z., Philpott, S.M., 2012. A meta-analysis of plant physiological and growth responses to temperature and elevated CO_2. Oecologia 169, 1–13.

Wang, Z., Jin, M., Šimůnek, J., van Genuchten, M. Th., 2014. Evaluation of mulched drip irrigation for cotton in arid Northwest China. Irrig. Sci. 32, 15–27.

Webb, L., Whetton, P., Barlow, E.W.R., 2007. Modelled impact of future climate change on phenology of wine grapes in Australia. Aust. J. Grape Wine Res. 13, 165–175.

Webb, L.B., Whetton, P.H., Barlow, E.W.R., 2011. Observed trends in wine grape maturity in Australia. Glob. Change Biol. 17, 2707–2719.

Webb, L.B., Whetton, P.H., Bhend, J., Darbyshire, R., Briggs, P.R., Barlow, E.W.R., 2012. Earlier wine-grape ripening driven by climatic warming and drying and management practices. Nat. Clim. Change 2, 259–264.

White, M.A., Whalen, P., Jones, G.V., 2009. Land and wine. Nat. Geosci. 2, 82–84.

Woznicki, S.A., Nejadhashemi, A.P., Parsinejad, M., 2015. Climate change and irrigation demand: uncertainty and adaptation. J. Hydrol: Reg. Stud. 3, 247–264.

Xiong, W., Holman, I., Lin, E., Conway, D., Jiang, J., Xu, Y., Li, Y., 2010. Climate change, water availability and future cereal production in China. Agric. Ecosyst Environ. 135 (1–2), 58–69.

Zhang, X., Walker, R.R., Stevens, R.M., Prior, L.D., 2002. Yield-salinity relationships of different grapevine (*Vitis Vinifera* L.) scion-rootstock combinations. Aust. J. Grape Wine Res. 8, 150–156.